

UKAEA-CCFE-CP(19)23

A. Krimmer, I. Balboa, N. J. Conway, M. De Bock, S. Frieze, F. Le Guern, N. C. Hawkes, D. Kampf, Y. Krasikov, P. Mertens, M. Mittwollen, K. Mlynczak, J. Oellerich, G. Szarvas, B. Weinhorst, C. Linsmeier

Design Status of the ITER Core CXRS Diagnostic Setup

This document is intended for publication in the open literature. It is made available on the understanding that it may not be further circulated and extracts or references may not be published prior to publication of the original when applicable, or without the consent of the UKAEA Publications Officer, Culham Science Centre, Building K1/0/83, Abingdon, Oxfordshire, OX14 3DB, UK.

Enquiries about copyright and reproduction should in the first instance be addressed to the UKAEA Publications Officer, Culham Science Centre, Building K1/0/83 Abingdon, Oxfordshire, OX14 3DB, UK. The United Kingdom Atomic Energy Authority is the copyright holder.

The contents of this document and all other UKAEA Preprints, Reports and Conference Papers are available to view online free at <https://scientific-publications.ukaea.uk/>

Design Status of the ITER Core CXRS Diagnostic Setup

A. Krimmer, I. Balboa, N. J. Conway, M. De Bock, S. Friese, F. Le
Guern, N. C. Hawkes, D. Kampf, Y. Krasikov, P. Mertens, M.
Mittwollen, K. Mlynczak, J. Oellerich, G. Szarvas, B. Weinhorst, C.
Linsmeier

Design Status of the ITER Core CXRS Diagnostic Setup

Andreas Krimmer^{a,*}, Itziar Balboa^b, Neil J. Conway^b, Maarten De Bock^c, Sebastian Friese^a, Frédéric Le Guern^d, Nick C. Hawkes^b, Dirk Kampf^e, Yuri Krasikov^a, Philippe Mertens^a, Martin Mittwollen^f, Krzysztof Mlynczak^a, Jan Oellerich^f, Gábor Szarvas^g, Bastian Weinhorst^h, Christian Linsmeier^a,

^aForschungszentrum Jülich GmbH, Institute of Energy and Climate Research, 52428 Jülich, Germany

^bUKAEA-CCFE, Culham Science Centre, Abingdon, Oxon, OX14 3DB, UK

^cITER Organization, Route de Vinon-sur-Verdon, CS 90 046, 13067 St. Paul Lez Durance Cedex, France

^dF4E - Fusion for Energy, 08019 Barcelona, Spain

^eKampf Telescope Optics GmbH, 81373 München, Germany

^fKarlsruhe Institute of Technology (KIT), Institute of Materials Handling and Logistics, 76131 Karlsruhe, Germany

^gOptimal Optik Kft., 1118 Budapest, Hungary

^hKarlsruhe Institute of Technology (KIT), Institute for Neutron Physics and Reactor Technology, 76344 Eggenstein-Leopoldshafen, Germany

Abstract

The Charge eXchange Recombination Spectroscopy diagnostic system on the ITER plasma core (CXRS core) will provide spatially resolved measurements of plasma parameters. The optical front-end is located in upper port 3 and the light of 460 nm to 665 nm is routed to spectrometers housed in the tritium building. This paper describes the layout of the optical system in the port plug, cell and interspace areas. The layout is a continuation of the developments described in [1] and takes into account changes in the design of the upper port plug, considerations for the system lifetime as well as internal and external tolerances on the optical chain. The layout was selected also with a number of additional criteria, including optical performance, radiation shielding, maintainability and robustness. A free-space optical chain was added to relocate the coupling of the light into the optical fibres to the port cell. As a new sub-system, a line-of-sight finder based on the back-illumination and imaging of apertures at pupils and masks at images was added. With the line-of-sight finder, the absence of an object with detectable edges is addressed, enabling determination of deviations within the optical chain. Where feasible, existing solutions for sub-systems such as the shutter were adapted to the layout. The current status of the implementation is discussed.

Keywords: ITER, Core Charge Exchange Recombination Spectroscopy, CXRS, diagnostic design, spectroscopy

1. Overview

The Charge Exchange Recombination Spectroscopy diagnostic system for the ITER core (CXRS core) captures light originating from the interaction of the diagnostic neutral beam (DNB) with the plasma. The light in the wavelength range of 460 nm to 665 nm is examined spectroscopically. CXRS core is the primary diagnostic system for toroidal plasma rotation (v_{tor}), core ion temperature (core T_i), relative Helium concentration (nHe/ne), Helium profile, and core concentration of He, Be, C, Ne and Ar. It also contributes to a number of other measurements. The presence of 0.6% Neon in the plasma is expected during the measurements in ITER. Recent experience at JET also shows the ability to measure in an ITER-like environment in the presence of He, Be and N [2]. CXRS core is not suitable to measure Z_{eff} as primary diagnostic system due to lifetime considerations. It is also only able to determine a lower bound of Z_{eff} as it is not able to measure the concentration of all elements. The newly added Visible Spectroscopy Reference System (55.E6, VSRS) is assumed to take over this measurement.

The system level considerations taken into account in the update of the diagnostic layout are discussed in chapter 2 and the resulting optical system is detailed. The mechanical implementation of the different sub-systems is discussed in chapter 3.

2. CXRS core system level design and optical layout

As a continuation of the CXRS core design described in [1], the system level layout was revised taking into account the results of the conceptual design review and changes in the surrounding components. On the system level, the following changes were implemented:

- The coupling of light into the fibres was relocated to the port cell
- A mirror chain was implemented in the interspace and bioshield
- A line-of-sight (LOS) finder was added to the system
- The mirror chain in the upper port plug (UPP) was revised

Termination of the fibres was relocated to the port cell to reduce radiation damage to the fibres, avoiding the need to replace

*Corresponding author

Email address: a.krimmer@fz-juelich.de (Andreas Krimmer)

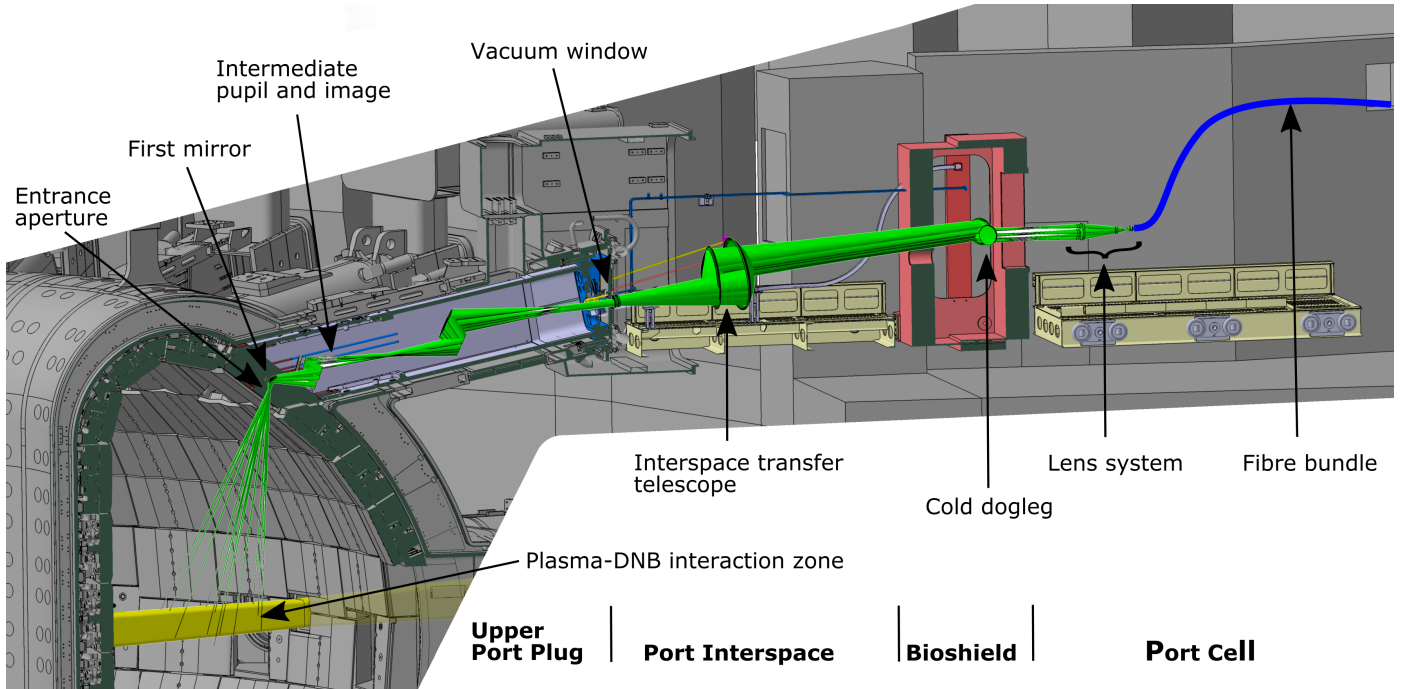


Figure 1: The CXRS core optical path and general set-up in the ITER UPP no. 3, port interspace and port cell.

the interspace section of the fibres. In addition, maintenance is simplified as the fibre length to be handled and stored during maintenance is minimized. The fibre positioning mechanism is also more accessible in the port cell.

To enable relocation of the fibres, an appropriate optical in-air chain of mirrors to transfer the light from the UPP to the port cell is implemented. Figure 1 gives an overview of the updated CXRS optical chain in port 3. In the interspace, a two-mirror transfer telescope is added. In the bioshield, a cold dogleg consisting of two flat mirrors is added. The lens system consists of 3 lenses (1 doublet) and focuses the beam onto the fibres. The last lens may be used to adjust focal length. The in-air optical chain is similar to the one proposed for the H-alpha diagnostic system.

The CXRS optical system implements an entrance pupil of 35 mm \varnothing at about 4.7 m distance to the object. For a field of 1.48 m times 0.49 m with a roughly trapezoid shape (see Figure 2), an étendue of 4.3×10^{-5} sr is transferred without vignetting. An initial transmission of around 40% in the relevant wavelength range from the object to the fibres is expected with a Rhodium first mirror (M1), Aluminium secondary mirrors in the UPP (M2-M5), protected Silver coating in-air, and the window and most lenses made from fused silica with AR coating on all surfaces. The magnification of the full optical chain is approximately 1/40.

2.1. Tolerances and deviations

The CXRS core nominal Field-of-View (FOV) extends from the geometric plasma centre to 1.4 m outwards, see Figure 2. The actual FOV, plasma position and DNB location are subject to assembly and operation tolerances which shift the target volume relative to the CXRS core FOV by ± 62 mm along the DNB

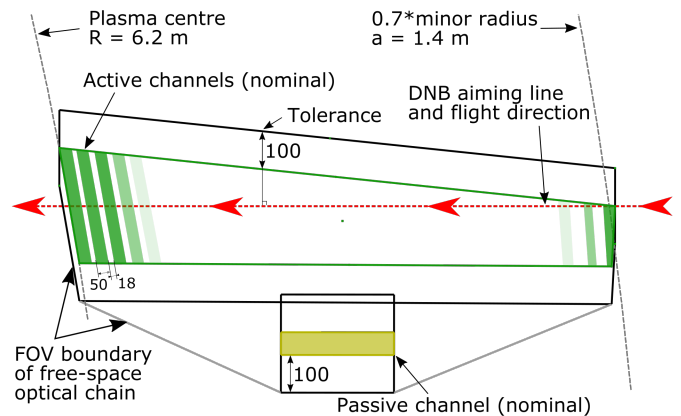


Figure 2: Field of view of the CXRS core diagnostic system.

flight direction, ± 152 mm across toroidally and ± 128 mm in focal depth of the CXRS core system. These numbers are a worst-case sum for the individual tolerances as currently known.

The FOV of the optical chain is designed to be adjusted by ± 100 mm across the DNB and ± 50 mm along the DNB flight direction during system assembly. This adjustment is realised by aligning the entrance aperture, first and second mirror. It can only take into account as-built deviations known at the time of assembly. No compensation of the focal length is planned as the loss of spatial resolution is limited.

To compensate for the deviations unknown at assembly time, the FOV extends beyond the nominal diagnostic channels by ± 100 mm in plasma toroidal direction. The area relevant to the diagnostic is selected at the coupling to the fibres in the port cell. No extension of the FOV is planned along the DNB flight

direction. In presence of deviations in this direction, CXRS core will lose 1 to 2 diagnostic channels in either the geometrical centre of the plasma or at the overlap to the edge CXRS system. With the tolerances as given, the diagnostic purpose can still be fulfilled.

The telescope on the Interspace Support Structure (ISS) is able to cope with ± 10 mm displacement and $\pm 0.5^\circ$ tilt (horizontal and vertical) of the beam coming from the UPP without repositioning, possibly sufficient for all deviations during plasma pulses. An initial positioning during assembly is required. Any deviations are relayed to the mirrors of the cold dogleg in the bioshield, which are equipped with active tip-tilt adjustment. They are used to compensate the movement of the beam, providing a stable and nominal position of the field on the lens system in the interspace.

In order to drive the cold dogleg mirrors, a measurement of the deviations in the optical path is necessary. As there is not object with detectable edges for the CXRS core system or even any specific light when the DNB is off, a specialised line-of-sight (LOS) finder is implemented. By back-illuminating the optical chain from the port cell, dedicated apertures of subsequently smaller size at pupils and masks at intermediate images with reflecting backsides are rendered observable. The masks are placed within the field at locations that do not take part in the diagnostic measurements. An imaging system coupled into the field in the port cell can then be used to detect the relative shifts between the pupil apertures (and masks after refocussing). With the shifts of apertures and masks, the relative location of the UPP, interspace telescope and lens system are calculated and then compensated for by the bioshield mirrors.

2.2. System lifetime

The system lifetime was maximised by the layout based on the criteria established by tests and simulation [3][4]. The entrance aperture size was reduced from $\varnothing 45$ mm to $\varnothing 35$ mm. In addition the distance between the entrance aperture and M1 was maximised, reaching 210 mm.

A cleaning system is planned for the first mirror. Research into first mirror cleaning is progressing [5] and implementation for CXRS core awaits definition of the cleaning system parameters. To allow effective cleaning without damaging the second mirror by the debris, the distance between M1 and M2 was maximised in the optical layout.

Lifetime is further increased by a shutter which follows the DNB operation cycle with the nominal cycle of 3 s on and 20 s off. The shutter is opened in time for the DNB pulse to start and closed immediately afterwards within < 1 s to maximise system lifetime. In case of a modified DNB duty cycle, the lifetime budget of the diagnostic system can be redistributed in accordance with the measurement needs.

To detect the degradation of the mirrors, a calibration system monitoring relative and absolute transmission of the optical chain is included. The UPP calibration system components are described in more detail below.

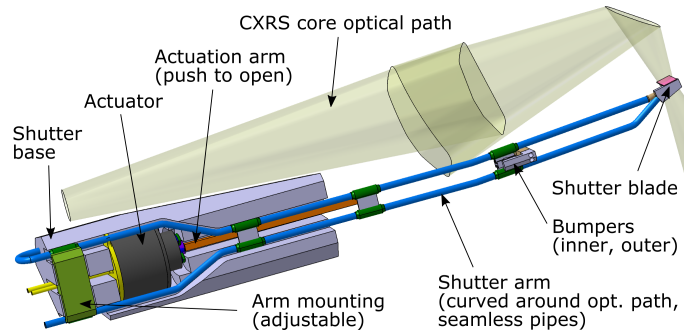


Figure 3: Preliminary shutter assembly, adopted to the updated optical layout.

3. UPP sub-systems implementation

3.1. Shutter

A shutter system for CXRS core is described in [6]. This shutter features two 2.1 m long arms and a per-arm blade travel distance of 24 mm with open and close times of 0.7 s. The shutter blade closes the optical path just behind the entrance aperture. It is placed after the aperture to allow use of the back-side as diffuse reflecting light source for calibration. Assuming optimistic 30,000 plasma pulses of 500 s duration and a DNB cycle duration of 23 s, a shutter cycle count of 660,000 is required.

This shutter with mock-up arms was successfully tested to 1,000,000 open-close cycles in air. No additional external loads outside of some baking cycles were applied during this testing. The actuator did not develop any defects or leaks. Limited wear was found at the dummy bumpers that limit shutter movement, but the functionality was not affected. A second shutter prototype with a detailed version of the shutter arm was tested to 1,000,000 cycles in vacuum without defects or leaks.

Experimental tests using a simplified parametric shutter mock-up showed that with accurate control of the pressure evolution, rebounds on the bumper could be completely suppressed without considerable vibrations of the blade [7].

With the changes to the optical layout, the shutter layout was modified, see Figure 3. Instead of two arms, only one arm can be used due to spatial limitations. The shutter provides a blade travel distance of 42 mm and requires a pressure of 4 bar absolute to open and pre-load against the bumpers. The open and close time of 0.7 s is kept. The shutter is mounted to the mid-plane of the UPP diagnostic shielding module (DSM), which is designed by the European port integrator to be assembled from two halves. The actuator and arm are mounted together on a common base structure to ease maintenance and allow accurate adjustment of the shutter blade location. The implications of the ancillary components necessary for driving the shutter (safety valves, compressor, tanks) are being checked.

3.2. In-vacuum mirrors

The first mirror (M1) may be attached to the front of the DSM, see Figure 4. It takes part in adjusting the FOV and can be aligned in piston and tip/tilt. A thin plate of single crystal Rhodium is chosen as mirror surface material based on corrosion resistance and reflectivity, with nano-crystalline Rh

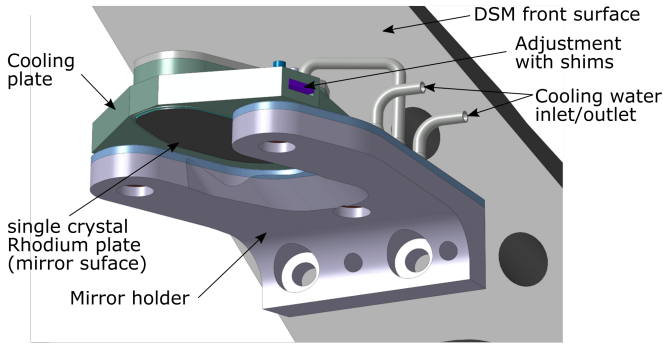


Figure 4: M1 attached to the front of the diagnostic shielding module.

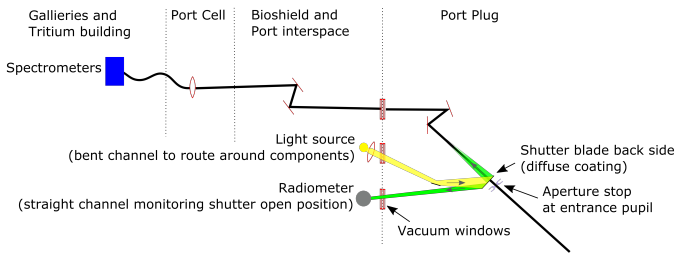


Figure 5: Scheme of the transmission calibration after assembly in the Tokamak.

coating as backup. Because of the high gamma heating of the Rhodium at the M1 location (average of around 70 W cm^{-3} , the mirror assembly is actively cooled. Details of the M1 substrate choice and design can be found in [8]. Maintenance of the mirror is planned as replacement of the complete assembly, with hands-on pre-aligning of the replacement against the surveyed as-aligned initial M1.

For the in-port mirrors 2 to 5, Aluminium was chosen as surface material. The substrate of M2 (dimension of 350 mm times 210 mm) and M3 are made from aluminium RSA-905 [9] and will be Al-coated to maximise reflectivity. With a measured electrical resistivity of $7.75 \times 10^{-8} \Omega \text{ m}$ at 70°C for RSA-905, the loads during disruptions are roughly cut in half compared to Al 6061-T6. At an estimated peak moment of 0.95 kNm during a Vertical Disruption Event (VDE-II lin 36 ms) with a reasonably light-weighted design, mounting of the substrate is still demanding.

3.3. UPP calibration system

As part of the diagnostic calibration, a set-up to measure the transmission of the optical chain in between pulses is foreseen to be implemented in the UPP. The system is based on illumination of the diffuse coated back-side of the shutter blade with a white light source. The absolute spectral radiance of the diffuse surface is measured directly with a radiometer and through the main optical chain. Both light source and radiometer are located in the port interspace with a channel to the shutter blade. An overview is given in Figure 5.

3.4. LOS finder

Inside the UPP, at least two apertures at pupils (the $\varnothing 35 \text{ mm}$ entrance pupil and intermediate pupil after M3) and a mask at

an intermediate image are foreseen to be implemented with diffuse reflecting properties and distinct shapes to allow identification of the elements of the LOS finder image. The size of the second aperture is chosen oversized to the system stop, but with a $\varnothing 10 \text{ mm}$ smaller than the UPP vacuum window (6 mm at the magnification of the window).

4. Conclusions

The CXRS core diagnostic system implements an optical system with relatively large FOV and high étendue given the narrow design space in the UPP and externally imposed tolerances. The optical layout was updated successfully improving system lifetime, incorporating tolerances from manufacturing and operation, and changes in the surrounding components. A design for the CXRS components in the UPP was proposed and many of the existing solutions from the previous layout could be incorporated.

Prototypes of the unmodified shutter have been successfully tested to 1,000,000 cycles. The full prototype did not show any significant damage and no leaks were found.

Detailing of the UPP diagnostic component is progressing and design of the ex-vessel components has started.

Acknowledgement

This work was supported by Fusion for Energy under the Framework Partnership Agreement F4E-FPA-408. The views and opinions expressed herein reflect only the author's views. Fusion for Energy is not liable for any use that may be made of the information contained therein.

References

- [1] Ph. Mertens, D. A. Castaño Bardawil, T. Baross et al., Status of the R&R activities to the design of an ITER core CXRS diagnostic system, *Fusion Engineering and Design* 96-97 (2015), proceedings of the 28th Symposium On Fusion Technology (SOFT-28).
- [2] N. Bonanomi, P. Mantica, A. D. Siena et al., Turbulent transport stabilization by ICRH minority fast ions in low rotating JET ILW L-mode plasmas, *Nuclear Fusion* 58 (5) (2018).
- [3] A. Litnovsky, M. Matveeva, L. Buzi et al., Studies of protection and recovery techniques of diagnostic mirrors for ITER, *Nuclear Fusion* 55 (9) (2015) 093015.
- [4] V. Kotov, Engineering estimates of impurity fluxes on the ITER port plugs, *Nuclear Fusion* 56 (10) (2016).
- [5] L. Moser, L. Marot, R. Steiner et al., Plasma cleaning of ITER first mirrors, *Physica Scripta* 2017 (T170) (2017).
- [6] D. A. Castaño Bardawil, Ph. Mertens, G. Offermanns et al., Design overview of the ITER core CXRS fast shutter and manufacturing implications during the detailed design work, *Fusion Engineering and Design* 96-97 (2015), proceedings of the 28th Symposium On Fusion Technology (SOFT-28).
- [7] S. Friese, A. Panin, Y. Krasikov et al., Experimental and numerical studies of the shutter dynamics for the ITER core CXRS diagnostic, *Fusion Engineering and Design* 123 (2017), proceedings of the 29th Symposium on Fusion Technology (SOFT-29) Prague.
- [8] Ph. Mertens, S. Dickheuer, Yu. Krasikov et al., On the use of rhodium mirrors for optical diagnostics in ITER, *Proc. 30th SOFT* (this conference), submitted to *Fusion Eng. Des.*
- [9] RSP technology, <http://www.rsp-technology.com>